Eur. J. Biochem. 207, 125–134 (1992)

Fluorescence study of the macrolide pentaene antibiotic filipin in aqueous solution and in a model system of membranes

Miguel A. R. B. CASTANHO and Manuel J. E. PRIETO
Centro de Química Física Molecular, Lisboa, Portugal

(Received January 23/March 20, 1992) – EJB 92 0091

The polyene antibiotic filipin (a pentaene) has been studied using photophysical techniques. The polyene self-aggregates in water with a critical micellar concentration of 2 μM. Two approaches were used to evaluate the aggregate dimensions: (a) a lower limit of 10 nm for the aggregate radius was obtained from energy transfer experiments; (b) a formula for rationalizing the turbidity spectrum was derived, and from its application a spherical shape of radius about 50 nm was deduced.

The low value for the fluorescence anisotropy of the aggregate ($r = 0.02$) is compatible with a very loose structure, i.e. the chromophore has very efficient depolarization dynamics that is not controlled by the aggregate size.

The Stern-Volmer plot of aggregated filipin fluorescence quenching by iodide is non-linear, presenting a downward curvature. A model was used for the interpretation of these data, along with a study of the quenching in transient state; it was concluded that all the components of the decay are affected by the quencher, i.e. the aggregate has a very open structure with respect to the iodide ion.

The partition constants of the polyene, K_p, between a model system of membranes (small unilamellar vesicles of dipalmitoylglycerophosphocholine) and the aqueous phase were determined from anisotropy measurements; the values obtained were K_p (gel phase) $= (3.4 \pm 0.8) \times 10^3$ and K_p (liquid crystal phase) $= (7.7 \pm 2.2) \times 10^2$. The observation that the polyene incorporation is efficient is at variance with the belief that the presence of sterols are essential for the interaction of polyene antibiotics with membranes [for review see Bolard, J. (1986) *Biochim. Biophys. Acta 864*, 257–304].

Filipin is a pentaene macrolide antibiotic with antifungal properties. Its biochemical mode of action is not certain but, in the two models proposed for its interaction with membranes [1, 2], the presence of sterols is reported to be an essential factor (for review see [3]); most of the studies of its toxicity were carried out in the presence of sterols (for review see [4]). The early work of Demel et al. [5], reporting that filipin does not penetrate monolayers of several lipids in the absence of sterols, and studies by freeze-etching techniques [6, 7], where no ultrastructural modifications were observed, reinforced the belief that the direct lipid–filipin interaction is not significant.

In spite of the intrinsic fluorescence of filipin, studies involving this technique are very few, its emission properties only being used to evaluate its interaction with sterols [8]. It is the purpose of the present work to report structural information on filipin, both in aqueous solution and when in interaction with a sterol-free model system of membranes (small unilamellar vesicles of L-α-1,2-dipalmitoyl-3-*sn*-glycerophosphocholine, $Pam_2GroPCho$) using photophysical techniques. The problems addressed were: (a) its aggregation in buffer and the dimension of the aggregate; (b) information on the aggregate structure from a fluorescence quenching study with iodide, both by transient and steady-state techniques (for the data analysis a model is presented considering the fluorophore complex decay); and (c) the incorporation in the membrane and the rotational dynamics of the filipin when in the membrane.

Correspondence to M. J. E. Prieto, Centro de Química Física Molecular, Complexo I–I. S. T., Av. Rovisco Pais, P-1096 Lisboa codex, Portugal

Fax: + 351 1 3524372.

Abbreviations. The indocarbocyanine, 1,1′-dioctadecyl-3,3,3′,3′-tetramethylindocarbocyanine perchlorate; $Pam_2GroPCho$, L-α-1,2-dipalmitoyl-3-*sn*-glycerophosphocholine.

MATERIALS AND METHODS

Most of the materials, experimental procedures and instrumentation for absorption and steady-state fluorescence were described recently [9]. Turbidity measurements were carried out with 10-cm cuvettes. In the iodide-quenching experiments, $Na_2S_2O_3$ (Merck) was present in order to avoid formation of I_2 and hence I_3^-.

From the reported relative fractions of filipin [10] (and an estimation of the molecular mass of the heaviest components), an average molar mass of 652 g/mol was calculated and will be used throughout this work, this value being close to that of filipin III (654 g/mol; Fig. 1).

1,1′-Dioctadecyl-3,3,3′,3′-tetramethylindocarbocyanine perchlorate (referred to as the indocarbocyanine) was supplied by Molecular Probes Inc. (Eugene, Oregon) and Triton X-100 by BDH (London, GB).

Multilamellar vesicles were disrupted to small unilamellar vesicles by sonication (Branson, 40 W), until no significant decrease in the scatter intensity of the suspension was observed (30 min). The vesicles were annealed for 10 min at 50 °C, to

decrease structural defects in the bilayer which could otherwise induce its fusion, and then submitted to low-speed centrifugation to separate titanium particles arising from the sonication.

Energy transfer efficiency was determined from the decrease of filipin emission ($\lambda_{exc.} = 338$ nm, $\lambda_{em.} = 480$ nm).

The single-photon timing technique was used to determine the fluorescence lifetimes as described in detail elsewhere [9]. In all cases, 10^4 counts were accumulated in the peak channel while background noise was usually less than 5 counts.

Fluorescence decays were, in general, complex and described by a sum of two or three exponentials, the mean lifetime, $\bar{\tau}$, being obtained from Eqn (1):

$$\bar{\tau} = \Sigma a_i \tau_i^2 / \Sigma a_i \tau_i . \quad (1)$$

The critical radius of transfer, R_0, was evaluated from Förster's formula, as described in [11].

RESULTS

Absorption and fluorescence spectra: photophysical parameters

The absorption and emission spectra of filipin in the presence of lipid membranes (small unilamellar vesicles of Pam$_2$Gro*P*Cho) is shown in Fig. 2. Except for a variation in the molar absorption coefficients (Table 1), these spectra are identical to those of monomeric or aggregated filipin in Tris buffer [9]. The expected vibrational progression of a polyene chromophore (≈ 1570 cm^{-1}) is observed as well as a large Stokes shift.

A plot of the fluorescence intensity of filipin versus concentration in buffer is presented in Fig. 3. Biphasic behaviour is observed with a transition at 2 μM, indicating the formation of an aggregate with a quantum yield greater than that of the monomer.

The molar absorption coefficient (ε), the quantum yield (ϕ_f) and the steady-state anisotropy (r) of filipin in the presence of lipid and of the monomeric and aggregated species in buffer are presented in Table 1.

In Fig. 4, the variation of fluorescence quantum yield, ϕ_f, versus antibiotic concentration is shown. Upon formation of the aggregate, the quantum yield increases and reaches a plateau.

Except for the monomer in buffer and filipin in the solid state, lifetimes for this antibiotic are complex, as shown in Table 2. When in interaction with the lipid, two exponentials are needed to describe the decay and, to fit the aggregate fluorescence decay in buffer, a third component of about 1 ns must be invoked.

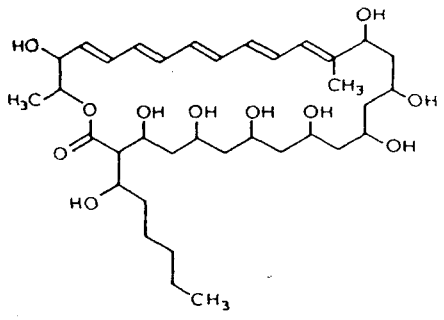

Fig. 1. Molecular structure of filipin III.

Light scattering: modified turbidity spectrum

The aggregate dimensions were accessed by studying the scattered light at various wavelengths. The pseudo-absorption, A', due to the scattered light in a transmission geometry, can be related to the external (b) and internal (a) radii of the aggregate via Eqn (2), where $[F]_t$ and Q are the total filipin molar concentration and the dissipation factor, respectively (Appendix I).

$$A' = 13.9\,(n\pi/\lambda)^4[(m^2-1)/(m^2+2)]^2(b^3-a^3)\,[F]_t\,N\,v\,Q \quad (2)$$

where $m = n_0/n$ is the relative refractive index, n_0 is the refractive index of the particle and n is that of the medium, N is Avogadro's number and v is the volume of the monomer. The refractive index of filipin was considered to be identical to that of Pam$_2$Gro*P*Cho [12], $n_0 = 1.116$; the volume, v, was determined using the method indicated in Appendix I.

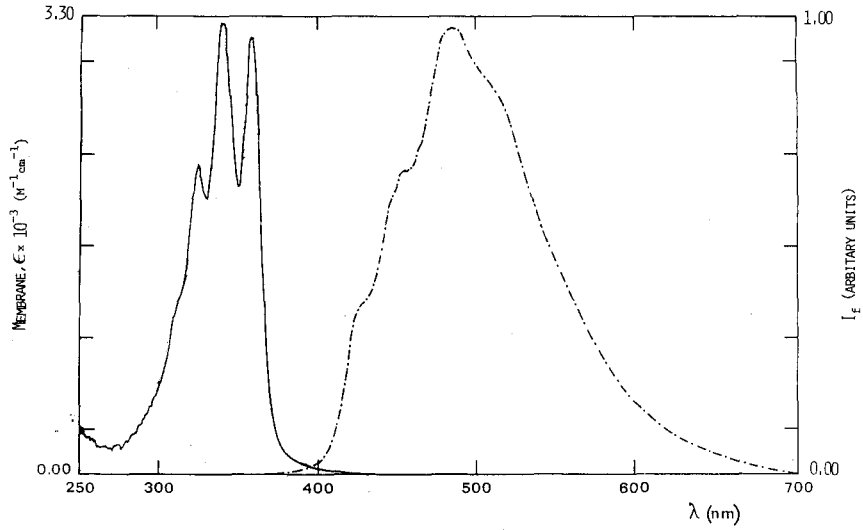

Fig. 2. Filipin absorption (——) and fluorescence emission (— · — · —), $\lambda_{exc} = 338$ nm) spectra in the presence of small unilamellar vesicles of Pam$_2$Gro*P*Cho (1 mM).

Table 1. Photophysical parameters for monomeric and aggregated filipin in buffer and in the presence of 1 mM $Pam_2GroPCho$. The molar absorption coefficient ε, fluorescence quantum yield ϕ_f (degassed solutions) and anisotropy r were measured.

Medium	Filipin state	Concn range	Temp.	ε	ϕ_f	r
		μM	°C	$M^{-1}\,cm^{-1}$		
Buffer	monomeric	0.01 – 1	25	4.7×10^4	0.08[a]	0.02[a]
Buffer	aggregated	6 – 20	25	4.7×10^4	0.26[a]	0.02[a]
Buffer + $Pam_2GroPCho$	—	0.1 – 50	25[b]	3.2×10^3	0.30	0.25
			45[c]	—	0.30	0.07

[a] Values from [1].
[b] Gel phase membranes (ε value is biased due to light scattering).
[c] Liquid crystal phase membranes.

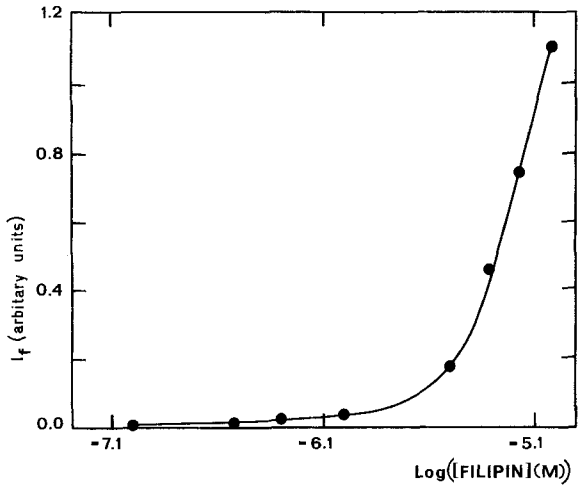

Fig. 3. Filipin fluorescence intensity (λ_{exc} = 338 nm, λ_{em} = 480 nm) versus concentration (log scale) in buffer at 25°C.

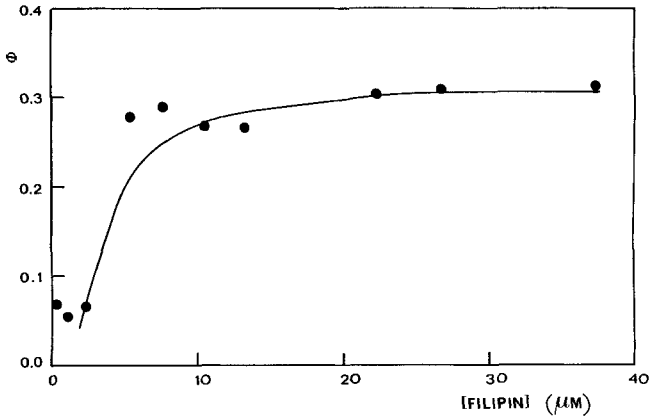

Fig. 4. Filipin fluorescence (λ_{exc} = 338 nm) quantum yield versus concentration. Fit of Eqn (6) to experimental data with $\phi_M = 0.08$ and $c_{cm} = 1$ μM (——).

The experimental result obtained for aggregated filipin in buffer is shown in Fig. 5, together with the theoretical expectation for an aggregate with an external radius of 53 nm and no empty core.

Energy transfer

Energy transfer measurements were carried out in order to determine the filipin aggregate dimensions. A model for energy transfer (dipolar mechanism, Förster type) in spherical geometry was derived previously [11]; its application enables the determination of the aggregate radii.

In this experiment filipin is the donor and the hydrophobic indocarbocyanine was chosen as an acceptor. The absorption spectrum of the cyanine in buffer red-shifts 3 nm when filipin is added to the system, demonstrating its interaction with the filipin aggregates. The Förster critical radius of transfer was determined for this donor/acceptor pair (R_o = 4.9 nm). No energy transfer was observed even for high acceptor concentrations up to 0.5 mM.

Fluorescence quenching studies

Filipin fluorescence in the aqueous phase was quenched by iodide ion. For the polyene monomer quenching, a linear Stern-Volmer relationship was obtained with a Stern-Volmer constant K_{sv} = 8.3 M^{-1}, as shown in Fig. 6. At variance with this result, a Lehrer-type Stern-Volmer plot (i.e. with a downward curvature) was obtained for the aggregate.

A transient-state quenching study was carried out. In a three-exponential free fit of the decay (six parameters), both the long (≈ 15 ns) and the medium (≈ 7 ns) components were affected. The short one (≈ 2 ns) was not significantly altered (Fig. 7). In this way, the two main components of the aggregate seem to be accessible to the quencher, so a significant non-accessible fluorescent population, as required for a Lehrer-type formulation, does not seems plausible.

Determination of the partition coefficient between the aqueous and lipid phases

The large variation of fluorescence anisotropy observed upon polyene incorporation in the membrane (Table 1), and the significant values of quantum yields in both phases, allow the partition coefficient of the antibiotic between the two phases to be obtained by studying the anisotropy variation.

The variation of filipin anisotropy upon increasing the lipid concentration, at 22°C and 46°C, is shown in Fig. 8. Above the phase-transition temperature, anisotropy increases and reaches a plateau. In the gel phase a sharp increase is observed and a maximum value is attained at concentrations of about 3 mM lipid. Beyond this concentration, the anisotropy decreases. This is thought to be due to the effect of light scattering, which is more relevant in the gel phase and at the higher lipid concentrations.

DISCUSSION

Absorption and fluorescence spectra: photophysical parameters

The absorption and emission spectra of filipin are those expected for a pentaene chromophore, namely the observed

Table 2. 'Best-fit' fluorescence decay parameters for filipin emission in degassed solutions. τ_i = lifetime of component i; a_i = pre-exponential factor of component i; $\bar{\tau}$ = mean lifetime. Measurements for filipin in the solid state were taken in a front-face geometry.

Medium	Filipin state	Concn range	Temp.	a_1	τ_1	a_2	τ_2	a_3	τ_3	$\bar{\tau}$
		μM	°C		ns		ns		ns	
–	solid	–	22	0.98	1.1	–	–	–	–	1.1
Buffer	monomeric	0.01 – 2	25	0.24	14.0	–	–	–	–	14.0
Buffer	aggregated	3 – 50	25	0.36	15.1	0.24	6.6	0.33	1.5	12.4
Buffer	aggregated	3 – 50	45	0.19	12.3	0.06	4.7	0.08	0.4	11.4
Buffer + 1 mM Pam_2 Gro*P* Cho	–	1 – 40	25	0.15	22.6	0.10	11.1	–	–	19.8
	–	1 – 40	45	0.19	16.1	0.11	7.1	–	–	14.3

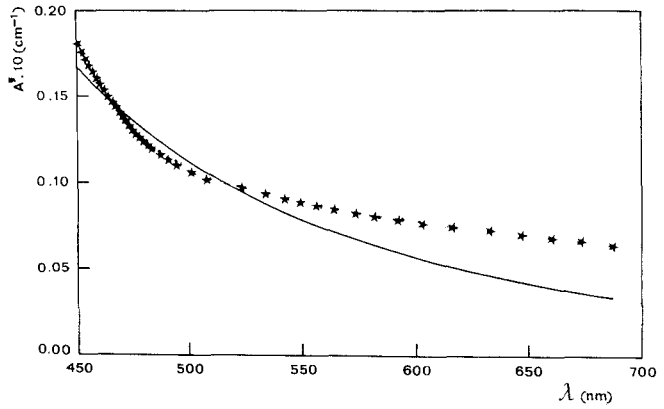

Fig. 5. Filipin (0.05 mM) modified turbidity spectrum in aqueous solution at 22°C. Fit of Eqn (2) to experimental data with a = 0 nm and b = 53 nm (——).

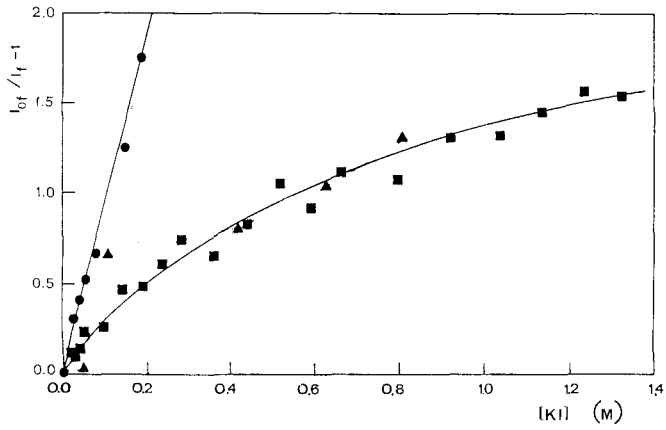

Fig. 6. Steady-state Stern-Volmer plot for the fluorescence quenching of filipin monomer (●) (0.7 μM) and aggregate (■) (0.04 mM) by iodide. Recovered Stern-Volmer plot (▲) from transient-state data (Eqn 10).

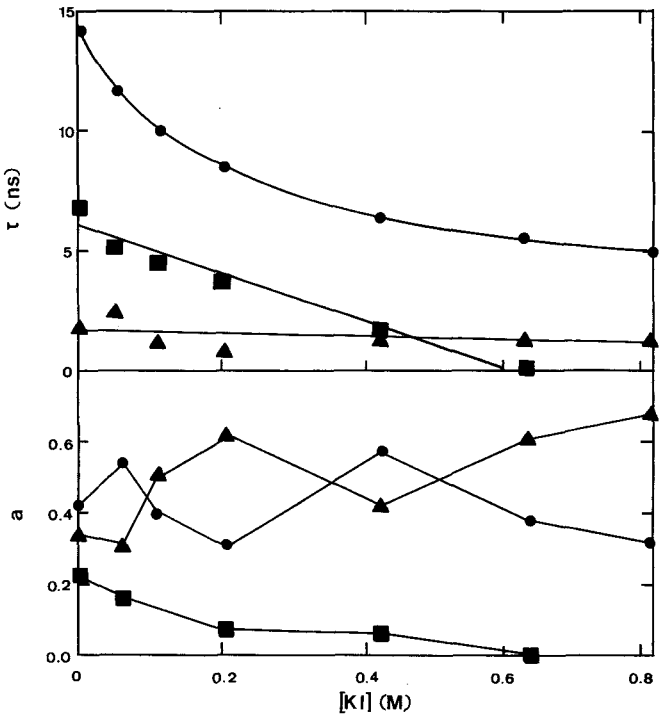

Fig. 7. Dependence of filipin (aggregate) fluorescence decay parameters (lifetimes, τ, and pre-exponential factors, *a*) on iodide concentration in aqueous solutions at 25°C. Solid lines are presented for clarity and have no physical meaning.

strong vibrational progression of the absorption and the large Stokes shift. Polyene photophysics is well described in the literature [13, 14]; the first singlet is a optically forbidden state ($^1A_g^*$), and the strong absorption arises from the allowed $^1B_u^* \leftarrow {}^1Ag$ transition (S_2). An all-*trans* pentaene chromophore has its longest wavelength absorption maximum at 334 nm [15]. Filipin absorption is red-shifted 23 nm due to the polyene interaction with a hydroxyl group (see Fig. 1).

Evidence for filipin aggregation in buffer is obtained from the fluorescence intensity versus concentration plot (Fig. 3), due to the large variation of quantum yield upon filipin aggregation (Table 1). The critical micellar concentration is clearly determined as 2 μM, this value being in agreement with the value of 1 μM obtained from light scattering measurements [9].

Filipin fluorescence excitation and emission spectra are insensitive to aggregation. This could indicate that the chromophore environment is not drastically changed. Although it is not possible, due to solubility problems, to carry out a study of solvent-induced spectral changes for this antibiotic, a spectral dependence on the polarizability has been reported for the tetraene *trans*-parinaric acid [16]. As no changes are observed upon antibiotic aggregation, no drastic alterations in the fluorophore environment can be inferred.

No evidence for exciton interaction, similar to that induced by cholesterol in the same system [9], is observed in the aggre-

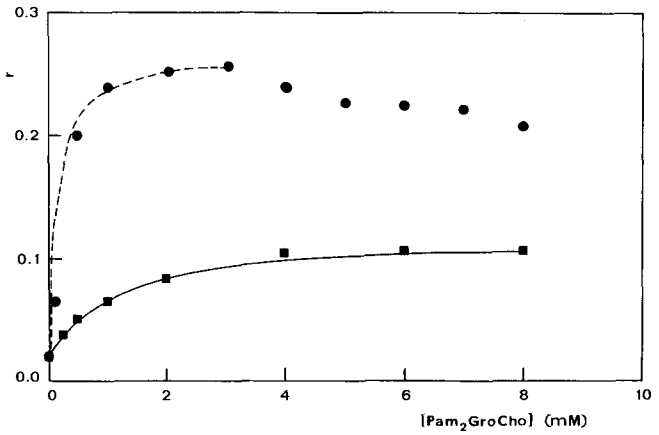

Fig. 8. Filipin fluorescence anisotropy versus lipid (small unilamellar vesicles of $Pam_2GroPCho$) concentration at 22°C (●) and 46°C (■). Fit of Eqn (12) to experimental data with (----) $K_p = (3.4 \pm 0.8) \times 10^3$ and $r_l = 0.29 \pm 0.02$ (gel phase) and (——) $K_p = (7.7 \pm 2.2) \times 10^2$ and $r_l = 0.12 \pm 0.1$ (liquid crystal phase). The experimental data obtained at 22°C, at higher $Pam_2GroPCho$ concentrations, are biased due to light scattering and were neglected.

gate absorption spectrum. This indicates that the interchromophoric distances and/or orientations are not as strict as in the other cases, indicating a loose structure for the aggregate. This is in agreement with the low value observed for the anisotropy (Table 1) of such a large aggregate (minimum radius of 10 nm, as will be shown from the energy transfer experiments). As the mean lifetime values of monomeric and aggregated species are similar (Table 2), and considering the molecular radii of the monomer and aggregate as 0.9 and 10 nm, respectively, an anisotropy ratio of r(aggregate)/r(monomer) = 19.6 should be obtained, from Perrin and Stokes-Einstein equations [17]. Contrary to these predictions, the value of anisotropy observed for the aggregate is very low and equals that of the monomer (Table 1). This reveals that the chromophore has efficient depolarization dynamics, the anisotropy not being controlled by the aggregate size. It should be stressed that, due to the large Stokes shift, energy migration is not operative and it does not affect the anisotropy. The low anisotropy value is thus rationalized on the basis of rotational freedom of the monomers within the structure of the aggregate, not on the rotation of the aggregate itself. So, the low value of anisotropy ($r = 0.02$) indicates a high degree of freedom of the monomers inside the aggregate.

The high value of anisotropy observed for the lipid-incorporated polyene reflects the strong immobilization induced by the membrane structure.

The variation of fluorescence quantum yield (Fig. 4) is compatible with the formation of a monodispersed aggregate of filipin (Eqn 3), where n is the aggregation number,

$$n\,F \rightleftharpoons F_n. \tag{3}$$

In this case, the filipin total concentration, $[F]_t$, is

$$[F]_t = [F] + n[F_n]. \tag{4}$$

When $[F]_t$ is greater than the critical micellar concentration, c_{cm}, then $[F] = c_{cm}$ and for the quantum yield, ϕ, Eqn (5) holds:

$$\phi = \phi_M[F]/[F]_t + \phi_A n[F_n]/[F]_t \tag{5}$$

or

$$\phi = \phi_A + c_{cm}(\phi_M - \phi_A)/[F]_t \tag{6}$$

where ϕ_A and ϕ_M are the aggregate and monomer quantum yields, respectively. Upon substitution of the experimental values for ϕ_M and c_{cm}, Eqn (6) qualitatively describes the experimental values presented in Fig. 4, a value of $\phi_A = 0.3$ being obtained from the best fit. We would like to stress that the existence of a polydisperse system cannot be ruled out by the present experiment.

The complex fluorescence decay of the antibiotic is also common to other polyenes. Monomeric parinaric acid fluorescence in protic solvents is monoexponential [18] and, when incorporated in membranes, most of the literature agrees with a two-component decay for this chromophore [19]. The longer component has been ascribed to the probes in the gel phase and the shorter one to a population of molecules in liquid crystalline domains that exist below the phase-transition temperature. For filipin we obtained an identical behaviour, i.e. a monoexponential decay for the monomer and a biexponential decay for the polyene in the membrane. At this stage it is not possible to assign the decays to populations in known environments; at variance with parinaric acids [19], we noticed that the lifetime of the monomeric filipin (τ = 14 ns) is quite long and similar to the mean lifetime in the membrane. On the other hand, a significant decrease of $\bar{\tau}$ in the liquid crystalline state is not observed and the quantum yield is invariant with the phase transition.

The fluorescence decay of the aggregate in buffer presents, in addition to the 15-ns component (similar to the monomer), two additional faster components of 7 ns and 2 ns. We are aware that the three discrete lifetime components eventually describe a continuous distribution of lifetimes [20]. The maximum entropy method [21] could also be used to characterize the decay without model assumptions regarding the distribution function.

Light scattering: modified turbidity spectrum

As shown in Appendix I, after the derivation of the formalism for the turbidity spectrum, the method was tested by application to a well described micelle, Triton X-100; a largely satisfactory agreement was obtained. When this methodology was applied to the filipin aggregate, a much poorer fit was observed (Fig. 5), but an approximate dimension for the aggregate can be obtained, about 50 nm. This value should be an upper limit as the filipin aggregate seems not to be compact, as assumed in Eqn (AI.9) in Appendix I. The large deviation obtained between theoretical expectation and experimental results (Fig. 5) might indicate a certain degree of polidispersity (in size and/or shape) of the system. Some sensitivity to the aggregate shape (contained in the dissipation factor, Q) is also obtained; for example, the fit for a rod (formulae derived in a similar way to Appendix I) is much worse, and the best results are obtained with a rod length that is close to the diameter of its sectional area (and similar to double the radius obtained assuming a sphere), so the aggregate seems to be close to spherical. Although detailed information cannot be obtained, the light scattering experiments clearly indicate that the aggregate is quite large; it will be shown that this conclusion is supported by the energy transfer experiment.

Energy transfer experiments

We observed no filipin fluorescence quenching by the indocarbocyanine. This could arise from segregation of the indocarbocyanine, i.e. this probe would self-aggregate and it would not be incorporated into the filipin micelles. This is ruled out by the red-shift of 3 nm observed, which is a known

response of the absorption spectrum of dyes upon incorporation into micelles [22].

A negative result of energy transfer contains information on distances between donor and acceptor; once the theoretical efficiency for a donor/acceptor pair is determined, a lower boundary of distance can be obtained. The absence of energy transfer in the efficient system (R_o = 4.9 nm) under study is rationalized on the basis of a large radius for the aggregate. Even if a lower limit is considered, e.g. only a 10% reduction of donor intensity is observed (this underestimates largely the experimental sensitivity), the condition $R \approx R_o/0.5$ (R is the sphere radius) would be obtained as inferred from a model of energy transfer in spherical geometry [11]. In this way, we can safely conclude a lower limit of $R \approx 10$ nm for the filipin aggregate radius, in qualitative agreement with the conclusions obtained from light scattering experiments. It is worth noting that, if the other experimental limit was verified, $R < 2.5\ R_o$, complete quenching would be obtained; in this situation, the aggregation number for the aggregate could be determined from the Turro and Ietka procedure [23].

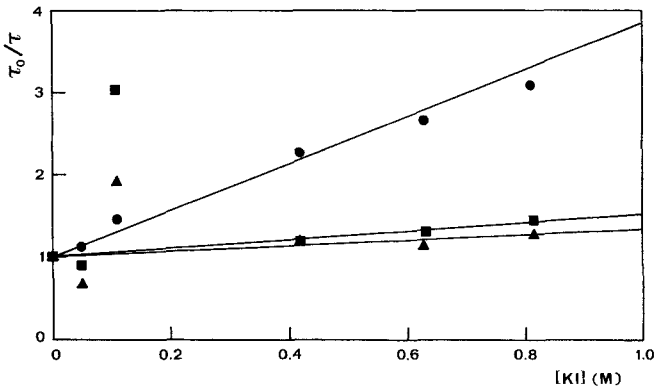

Fig. 9. Stern-Volmer plot (transient state) for the quenching of filipin aggregate (0.04 mM) by iodide. Fluorescence decays were analysed according to Eqn (9), with V = 1.8 nm^3. (●) Long component; (■) medium component; (▲) short component.

Fluorescence quenching studies

Quenching of filipin monomer fluorescence was, as expected, described by a linear Stern-Volmer relationship (Fig. 6). When determining the value obtained for the bimolecular rate constant of fluorescence, $k_q = 5.9 \times 10^8$ M^{-1} s^{-1}, and using this in the Smoluchovski relationship (Eqn 7) with the diffusion coefficient $D = 5.65 \times 10^{-8}$ cm^2 s^{-1} for filipin, a low efficiency parameter, $\gamma = 0.05$, is obtained.

$$k_q = \gamma 4\pi N R_{pq} D_{pq} . \qquad (7)$$

γ is the efficiency parameter, R_{pq} is the collision radius (taken as the sum of the Van der Walls radii) and D_{pq} is the sum of fluorophore and quencher diffusion coefficients. The fluorophore diffusion coefficients were obtained from the Stokes-Einstein relationship, the addition of atomic radii being considered to evaluate the molecular volume [24]. The experimental value for iodide diffusion is $D = 1.90 \times 10^{-5}$ cm^2 s^{-1} [25].

For the filipin aggregate a Lehrer-type quenching plot (i.e. with a downward curvature) was obtained (Fig. 6). As the decay is complex, with short (τ = 1.5 ns), medium (τ = 6.6 ns) and long (τ = 15.1 ns) components, information on the quenching kinetics should also be obtained by transient-state techniques. Due to the large number of parameters (six) involved in transient-state data analysis, a model was used to analyse it. We assumed that if the decay without quencher is described by Eqn (8):

$$I(t) = \sum_{i=1}^{3} (a_i e^{-t/\tau_i}) \qquad (8)$$

where $I(t)$ is the fluorescence intensity at instant t, a_i is the pre-exponential factor for component i and τ_i is the lifetime component of i, then, in the presence of quencher, the following relationship would hold (Eqn 9):

$$I(t) = \sum_{i=1}^{3} (a'_i e^{-t/\tau'_i}) = \sum_{i=1}^{3} (a_i e^{-V_i[Q]N\gamma} e^{-t/\tau'_i}) \qquad (9)$$

where V_i is the volume of the sphere of action of component i, [Q] is the quencher molar concentration, N is Avogadro's number, τ'_i is the lifetime component of i in the presence of the quencher at concentration [Q] and γ is the efficiency parameter of quenching. Thus the static contribution would be described by a sphere of action formalism [17] (demonstration that the efficiency parameter, γ, should be included in the exponential term is presented in Appendix II). V_i and [Q] were considered identical for all the components and, in this way, the fit was reduced to four parameters: the volume, V, and the three lifetimes. The efficiency parameter, $\gamma = 0.05$, is known from the monomer quenching study and was considered identical for all the components. The variation of the lifetimes, from τ_i to τ'_i, contains information on the dynamic quenching process.

In addition, the steady-state quenching Stern-Volmer plot should be obtained from Eqns (8) and (9) upon integration (Eqn 10):

$$I_o/I = \sum(a_i \tau_i)/\Sigma(a'_i \tau'_i) . \qquad (10)$$

The best fit was found with a value of V = 1.8 nm^3, corresponding to a radius of 0.8 nm, this value being close to the sum of chromophore and quencher molecular radii. The recovered lifetimes of the components are shown as a Stern-Volmer plot in Fig. 9. The overall trend is satisfactory, i.e. linear Stern-Volmer plots are obtained, except for medium and short components at concentrations of [Q] = 0.11 M and [Q] = 0.05 M. In addition, the steady-state quenching plot is correctly described by Eqn (10), as shown in Fig. 6.

The complex decay of the fluorophore, i.e. the number of parameters involved, prevents the consideration of transient effects in diffusion [26] and no attempt was made to try to fit the decays in this assumption. This is not critical for the conclusions aimed at in this work.

From the dynamic quenching plot, Fig. 9, the bimolecular quenching rate constants of $k_q = 2.3 \times 10^8$ M^{-1} s^{-1} (short component), $k_q = 6.9 \times 10^7$ M^{-1} s^{-1} (medium component) and $k_q = 2.0 \times 10^8$ M^{-1} s^{-1} (long component) were obtained. All the values are quite similar, but it could be speculated that, for the medium component, the environment is slightly more viscous.

Altogether these results indicate that the aggregate is an open structure, all the fluorophores being accessible to iodide, excluding the existence of an hydrophobic core, which would be difficult to realize considering the amphipathic character of the filipin molecule. In addition, it was proved that a correct analysis of quenching in the case of complex decays, rules out an immediate Lehrer interpretation, invoking populations of fluorophores non-accessible to quenchers.

Determination of the partition coefficient between aqueous and lipid phases

The partition coefficient of a solute between the lipid and aqueous phases, K_p, is defined as

$$K_p = \frac{n_l/v_l}{n_w/v_w} \tag{11}$$

where n_i is the moles of solute in the lipid ($i = l$) or aqueous ($i = w$) phase and v_i are the volumes of these phases. As anisotropy is a parameter with additive properties and the anisotropies in each phase are clearly distinct, the measured anisotropy can be directly related to the partition coefficient, K_p (Appendix III):

$$r = \{[1/(\gamma_l[L]) - 1]r_w + r_l K_p \phi_l/\phi_w\}/[1/(\gamma_l[L]) - 1 + K_p \phi_l/\phi_w]. \tag{12}$$

In Eqn (12), r_i are the anisotropies in the lipid ($i = l$) or aqueous phase ($i = w$), ϕ_l/ϕ_w is the ratio between the fluorescence quantum yield of membrane-incorporated filipin and that in solution, γ_l is the molar volume of the lipid in the membrane and [L] is the molar concentration of $Pam_2GroPCho$. With ϕ_l and ϕ_w previously determined and $\gamma_l = 0.83$ dm^3/mol (gel phase) and $\gamma_l = 0.95$ dm^3/mol (liquid crystal), evaluated from data available in the literature [27], K_p and r_l were obtained from a non-linear regression fit of r vs [L].

The best fit obtained from Eqn (12) to the experimental results is shown in Fig. 8; it corresponds to values of K_p (gel phase) $= (3.4 \pm 0.8) \times 10^3$ and K_p (liquid crystal phase) $= (7.7 \pm 2.2) \times 10^2$, the anisotropies in the lipid being r_l (gel) $= 0.29 \pm 0.02$ and r_l (liquid crystal) $= 0.12 \pm 0.01$.

The concentration of filipin in the lipid is 4.4 ± 0.2 times greater in the gel phase than in the liquid crystal phase. This ratio is also the partition constant of the antibiotic between the two phases in a membrane system where both phases are present, i.e. filipin prefers the gel phase, such as observed for *trans*-parinaric acid, for which an identical ratio (3 ± 1) has been reported [28]. In addition, it should be stressed that filipin is incorporated into the membrane in the absence of cholesterol; this observation is at variance with the belief that sterols are essential for the interaction of the antibiotic with the membranes (see introduction and references therein).

Biochemical relevance of the results

Since it is released by bacteria, filipin, like all other polyene antibiotics, has to pass through aqueous media to reach the target membranes (e.g. fungal plasma membranes). The diffusive behaviour of filipin is not known, in spite of its key role in the biochemical mode of action of the antibiotic. Attention has been focused only on the final step of its biological action (the interaction with the target membrane). This study follows the preliminary studies of Lampen [29] in an attempt to clarify and characterize, from a biochemical point of view, the behaviour of polyene antibiotics in aqueous solution. The filipin aggregation (imposed by its amphipathic nature) is the main feature of this behaviour. The knowledge of the nature of the aggregate (large, loose and with all the molecules accessible to the solvent) is essential to understand the nature of antibiotic intermolecular interactions. The partition of the antibiotic between aqueous phase and lipid membranes (of importance to understanding the lytic action of filipin, its toxicity from a therapeutic point of view and its potential pharmaceutical advantages) can only be understood on the basis of a competition between antibiotic/antibiotic interaction and antibiotic/lipid interaction. The thermodynamic balance of this competition dictates the extent of incorporation of filipin into membranes, determining its biochemical and pharmaceutical role.

The partition of filipin into sterol-free membranes is a major drawback for the use of filipin as a therapeutic agent in humans. The low toxic selectivity of filipin was believed to be related to its inability to 'distinguish' between cholesterol (present in human cell membranes) and ergosterol (the major sterol in fungal plasma membranes); now this question has to be enlarged or reformulated.

The behaviour of filipin in aqueous solution has to be taken into account whenever pharmaceutical questions are being considered.

CONCLUSIONS

In this work we have studied the polyene antibiotic filipin by photophysical techniques, both in aqueous solutions and in interaction with a model system of membranes (small unilamellar vesicles of $Pam_2GroPCho$).

The critical micellar concentration (2 μM) was determined from the variation of fluorescence intensity with concentration; the dependence of fluorescence quantum yield on filipin concentration is compatible with a monodispersed distribution for the aggregate.

This aggregate was shown to be quite large. A lower limit of 10 nm for the aggregate radius was obtained from application of a model for energy transfer in spherical geometry; a formula for the analysis of turbidimetry spectra was derived, its application pointing to a spherical shape of about 50 nm radius. The low value of the fluorescence anisotropy of such a large aggregate ($r = 0.02$) is compatible with a loose structure, i.e. the chromophore depolarization dynamics are *not* controlled by the aggregate size.

The photophysical parameters quantum yield (ϕ_f), molar absorption coefficient (ε), anisotropy (r) and fluorescence lifetimes (τ) were obtained for filipin in interaction with a model membrane system and compared to the values for the monomer and aggregate in water. The aggregate is strongly fluorescent ($\phi_f = 0.26$), this value being similar to the one in the membrane. Except for the monomer ($\tau = 14$ ns), the decay of filipin aggregate (three components, $\tau_1 = 15.1$ ns, $\tau_2 = 6.6$ ns, $\tau_3 = 1.4$ ns), or for the antibiotic in the membrane (two components, $\tau_1 = 22.6$ ns, $\tau_2 = 11.1$ ns) are complex. Interestingly, no decrease of the quantum yield is observed upon gel-to-liquid phase transition and a significant decrease of the mean lifetime is not observed.

The aggregate is an open structure. A study of fluorescence quenching by iodide was carried out and all the components of the complex decay were shown to be quenched with similar efficiencies. For the analysis of the transient-state data a model was used, taking into account the contribution of a static mechanism of quenching, the steady-state quenching plot being correctly recovered from transient data.

The polyene fluorescence anisotropy increases when filipin interacts with a membrane (from $r = 0.02$ to $r = 0.25$, in gel phase, and to $r = 0.07$, in liquid crystal phase); its variation was used to determine the partition constant, K_p, between the two phases. Values of K_p (gel phase) $= (3.4 \pm 0.8) \times 10^3$ and K_p (liquid crystal phase) $= (7.7 \pm 2.2) \times 10^2$ were obtained. It is concluded that incorporation of filipin in a cholesterol-free membrane is quite efficient, at variance with the literature (see introduction and references therein), where the presence of sterol is considered essential. In addition, the ratio of partition

constants obtained, $K_p(\text{gel})/K_p$ (liquid crystal) $= 4.4 \pm 0.2$, is the partition constant between the two phases. This polyene prefers the gel phase, as does the tetraene *trans*-parinaric acid [28, 30].

APPENDIX I

Evaluation of an aggregate dimension from a modified turbidity spectrum

In the Rayleigh-Gans theory of light scattering, the intensity of light scattered at an angle θ (measured from the incident beam) by a solution with N' isotropic particles in a unit volume is [31]:

$$I(\theta)/I_o = N'/2\,(3\pi V'/r')^2(n/\lambda)^4[(m^2-1)/(m^2+1)]^2(1+\cos^2\theta)\,P(\theta) \quad \text{(AI.1)}$$

where $m = n_o/n$ is the relative refractive index, n_o is the refractive index of the particle and n is that of the medium, I_o is the intensity of incident light of wavelength λ and r' is the observation distance. $P(\theta)$ is the scatter factor and is a corrective parameter for the Rayleigh scattering, accounting for the interference of waves scattered from different sites of the particle [$P(\theta) \approx 1$ if $R_h \ll \lambda$, R_h being the particle hidrodynamic radius].

Integrating over the sphere of radius r' we obtain the total scattered light, S:

$$S = 24\pi^3 V'^2 N' I_o (n/\lambda)^4[(m^2-1)/(m^2+1)]^2 Q \quad \text{(AI.2)}$$

where Q is the dissipation factor:

$$Q = 3/8 \int_0^\pi [P(\theta)(1+\cos^2\theta)\sin\theta]\,d\theta. \quad \text{(AI.3)}$$

$P(\theta)$ equals the square of the form factor, f:

$$f = \frac{\int_0^\infty 4\pi r'^2 G(r')\sin(k'r')/(k'r')\,dr'}{\int_0^\infty 4\pi r' G(r')\,dr'} \quad \text{(AI.4)}$$

where $k' = 4\pi/\lambda \sin(\theta/2)$ and $G(r')$ is the radial distribution function.

For an empty sphere of internal radius a and external radius b (with an homogeneous distribution of scattering material):

$$P(\theta) = \left\{\frac{3[(\sin(k'b)-\sin(k'a)]/[k'+a\cos(k'a)-b\cos(k'b)]}{k'^2(b^3-a^3)}\right\}^2. \quad \text{(AI.5)}$$

If $b < \lambda/5$, a Taylor series expansion can be truncated to the first four terms with an error less than 9%. In this way we have:

$$Q = 1 + 15.79C_1/\lambda^2 + 8727.86(C_2/140 + C_1^2/100)/\lambda^4 + 773.51C_1C_2/\lambda^6 + 1639.44C_2^2/\lambda^8 \quad \text{(AI.6)}$$

where

$$C_1 = (a^5-b^5)/(b^3-a^3) \text{ and } C_2 = (b^7-a^7)/(b^3-a^3).$$

The turbidity is the total fraction of light that is scattered by the solution and is related to the pseudo-absorbance, A', measured in the spectrophotometer by a simple relationship (turbidity $= 2.303\,A'$) in dilute solutions. Eqn (AI.2) allows the evaluation of A':

$$2.303\,A' = 24\pi^3 V'^2 N' (n/\lambda)^4[(m^2-1)/(m^2+2)]^2 Q. \quad \text{(AI.7)}$$

As N' is the number of dispersing entities per unit volume, for monodispersed systems Eqn (AI.8) holds:

$$N' = ([M]_t - c_{cm})\,N/n_{agg} \approx [M]_t N v/V' \quad \text{(AI.8)}$$

where $[M]_t$ is the total molar concentration of the monomer, N is Avogadro's number, n_{agg} is the aggregation number and v is the monomer volume (which can be estimated from the method given in [24]).

V' is the volume of the aggregate that was assumed to be a sphere of internal radius a and external radius b, so (as long as the volume of the scattering material equals the volume of the sphere):

$$V' = 4\pi(b^3-a^3)/3. \quad \text{(AI.9)}$$

Sustituting Eqns (AI.8) and (AI.9) in (AI.7),

$$A' = 13.9\,(n\pi/\lambda)^4[(m^2-1)/(m^2+2)]^2(b^3-a^3)\,[F]_t N v Q. \quad \text{(AI.10)}$$

From a fit of the experimental turbidity spectrum to Eqn (AI.10), a and b can be determined.

This method was tested using Triton X-100 in conditions (50 mM Tris/HCl pH 8.0, 20°C) where it forms well known micelles with a geometry very close to spherical [32]. For the refractive index of the particle, a value identical to that of $Pam_2GroPCho$, $n_o = 1.116$, was considered [12]. Fig. AI.1 shows the experimental spectrum and the best fit, using Eqn (AI.10). This fit corresponds to an internal radius of 0 nm and an external one of 4.1 nm. Other techniques, cited in [32], yield values of 3.81 nm (small-angle X-ray scattering), 3.78 nm (inelastic light scattering) and 4.14 nm (diffusion techniques).

APPENDIX II

Static quenching (sphere-of-action)

If, at the moment of excitation, fluorophore and quencher are close enough, quenching of fluorescence may occur in an instantaneous way (static quenching). The sphere-of-action model [17] considers a sphere surrounding the fluorophore within which the probability of quenching is unity if there is at least one quencher molecule within this volume. However, if $\gamma < 1$ (γ is the efficiency parameter in Eqn 7), this does not hold because there is a probability that both molecules are in contact without reacting. In this way, the measured fluorescence intensity, I_f, is related to the fluorescence intensity in the absence of static quenching, $I_{f,o}$, by:

$$I_f = I_{f,o}\left[\sum_{i=0}^{N_t} P(i)\,P_{nq}(i)\right] \quad \text{(AII.1)}$$

where $P(i)$ is the probability of i molecules of quencher being located within a sphere of volume V, surrounding the fluorophore and $P_{nq}(i)$ is the probability of quenching not occurring once i molecules are within V, and N_t is the total number of molecules in solution.

Using the Poisson law for distribution of molecules in a volume:

$$P(i) = (V[Q]N)^i/i!\,e^{-V[Q]N} \quad \text{(AII.2)}$$

and once,

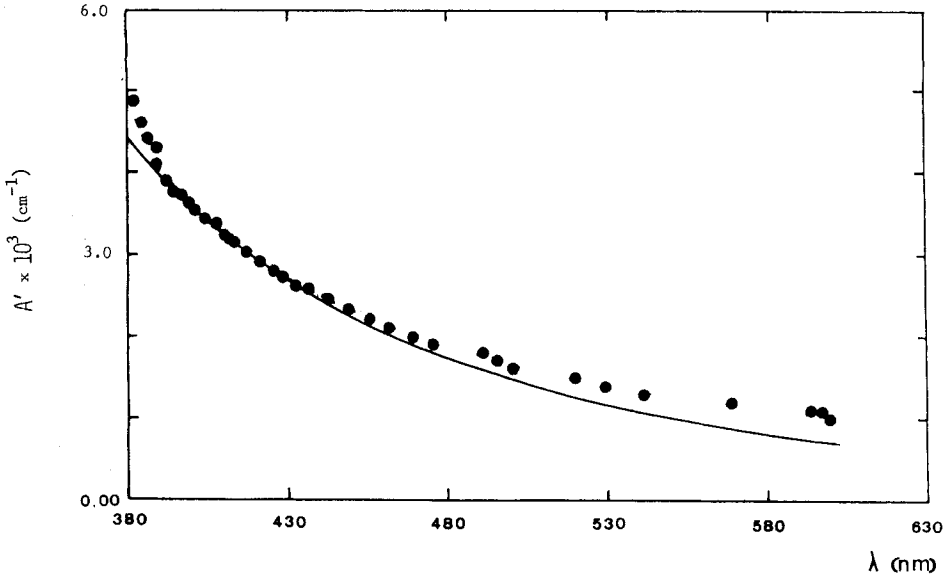

Fig. AI.1. Modified turbidity spectrum of Triton X-100 (●). (——) Fit of experimental data to Eqn (AI.10), with $a = 0$ nm and $b = 4.1$ nm.

$$P_{nq}(i) = (1-\gamma)^i. \qquad \text{(AII.3)}$$

Eqn (AII.1) is rewritten as:

$$I_f = I_{f,o}\, e^{-V[Q]N} \sum_{i=0}^{N_t} [(V[Q]N(1-\gamma))]^i/i!). \qquad \text{(AII.4)}$$

When $N_t \to \infty$:

$$\sum_{i=0}^{N_t} [(V[Q]N(1-\gamma))]^i/i!) \approx e^{V[Q]N(1-\gamma)}. \qquad \text{(AII.5)}$$

From Eqns (AII.5) and (AII.4):

$$I_f = I_{f,o}\, e^{-V[Q]N\gamma}. \qquad \text{(AII.6)}$$

Thus the static contribution is given by $e^{-V[Q]N\gamma}$. When $\gamma = 1$, the usual static term is obtained.

APPENDIX III

Determination of the partition coefficient between aqueous and lipid phase from anisotropy methods

Considering that the anisotropy, r, is an additive parameter [17],

$$r = \sum_i f_i r_i \qquad \text{(AIII.1)}$$

where r_i is anisotropy in aqueous phase ($i = w$) or in the lipid ($i = l$), and:

$$f_i = \varepsilon_i[F]_i \phi_i g_i / \sum_j (\varepsilon_j[F]_j \phi_j g_j) \qquad \text{(AIII.2)}$$

where ε_j is the molar absorption coefficient, ϕ_j is the quantum yield, $[F]_j$ is the molar concentration of the fluorophore and g_j is the fluorescence intensity at the emission wavelength in a normalized spectrum, this relationship being valid for dilute solutions. If g_j and ε_j are constant, Eqn (AIII.2) can be simplified to:

$$r = ([F]_w \phi_w r_w + [F]_l \phi_l r_l)/([F]_w \phi_w + [F]_l \phi_l). \qquad \text{(AIII.3)}$$

Then,

$$[F]_l/[F]_w = \phi_w/\phi_l (r_w - r)/(r - r_l). \qquad \text{(AIII.4)}$$

The molar fraction of fluorophore in the lipid phase, x_l, is:

$$x_l = \{(r_w - r)\phi_w/[(r - r_l)\phi_l]\}/\{(1 + (r_w - r)\phi_w/[(r - r_l)\phi_l]\}. \qquad \text{(AIII.5)}$$

Eqn (11) may be rewritten as:

$$K_p = [F]_l/[F]_w (1 - \gamma_l[L])/(\gamma_l[L]) \qquad \text{(AIII.6)}$$

where [L] is the molar concentration of the lipid and γ_l its molar volume.

Substitution of Eqn (AIII.6) into Eqn (AIII.4):

$$r = (D r_w + K_p Y r_l)/(D + K_p Y) \qquad \text{(AIII.7)}$$

where $D = 1/(\gamma_l[L]) - 1$ and $Y = \phi_l/\phi_w$.

So, r is a weighted mean value between r_w and r_l · r_w can be easly measured, r_l and K_p can be evaluated from a non-linear regression fit of Eqn (AIII.7) to experimental data.

This work was supported by *Instituto Nacional de Investigação Científica* (INIC, Portugal), project 1G-CQFM. M. A. R. B. C. acknowledges a grant from *Junta Nacional de Investigação Científica e Tecnológica* (JNICT, Portugal).

REFERENCES

1. De Kruijff, B. & Demel, R. A. (1974) *Biochim. Biophys. Acta 339*, 57–70.
2. Elias, P. M., Friend, D. S. & Goerke, J. (1979) *J. Histochem. Cytochem. 27*, 1247–1260.
3. Kinsky, S., Luse, S. & Van Deenen, L. (1966) *Fed. Proc. 25*, 1503–1510.
4. Bolard, J. (1986) *Biochim. Biophys. Acta 864*, 257–304.
5. Demel, R. A., Van Deenen, L. L. M. & Kinsky, S. C. (1965) *J. Biol. Chem. 240*, 2749–2753.
6. Tillack, T. W. & Kinsky, S. C. (1973) *Biochim. Biophys. Acta 323*, 43–54.
7. Verkleij, A. J., De Kruijff, B., Gerritsen, W. F., Demel, R. A., Van Deenen, L. L. M. & Ververgaert, V. (1973) *Biochim. Biophys. Acta 291*, 577–581.
8. Bittman, R. & Fischkoff, S. A. (1972) *Proc. Natl Acad. Sci. USA 69*, 3795–3799.
9. Castanho, M. A. R. B., Coutinho, A. & Prieto, M. (1992) *J. Biol. Chem. 267*, 204–209.
10. Bergy, M. & Eble, T. (1968) *Biochemistry 7*, 653–659.
11. Berberan-Santos, M. N. & Prieto, M. J. E. (1987) *J. Chem. Soc. Far. Trans. II 83*, 1391–1409.

12. Chong, C. S. & Colbow, K. (1976) *Biochim. Biophys. Acta 436*, 260–282.
13. Hudson, B. & Kohler, B. (1974) *Annu. Rev. Phys. Chem. 25*, 437–460.
14. Becker, R. S. (1988) *Photochem. Photobiol. 48*, 369–399.
15. Jaffé, H. H. & Orchin, M. (1970) *Theory and applications of ultraviolet spectroscopy*, 5th edn, pp. 220–241, John Wiley & Sons, London.
16. Sklar, A., Hudson, B. S., Peterson, M. & Diamond, J. (1977) *Biochemistry 16*, 813–819.
17. Lakowicz, J. R. (1983) *Principles of fluorescence spectroscopy*, Ch. 2, 5 and 9, Plenum Press, New York.
18. Wolber, P. K. & Hudson, B. (1981) *Biochemistry 20*, 2800–2810.
19. Hudson, B. & Cavalier, S. A. (1988) in *Spectroscopic membrane probes*, vol. I (Loew, L. M., ed.) pp. 43–62, CRC Press, Boca Raton FL.
20. James, D. R., Turnbull, J. R., Wagner, B. D., Ware, W. R. & Peterson, N. O. (1987) *Biochemistry 26*, 6272–6277.
21. Livesey, A. K. & Brochon, J. C. (1987) *Biophys. J. 52*, 693–706.
22. Diaz Garcia, M. E. & Sanz-Medel, A. (1986) *Talanta 33*, 255–264.
23. Turro, N. J. & Yetka, A. (1978) *J. Am. Chem. Soc. 100*, 5951–5952.
24. Edward, J. (1970) *J. Chem. Ed. 47*, 261–270.
25. Weast, R. C. (1971) *Handbook of chemistry and physics*, p. F47, The Chemical Rubber Co, Cleveland, Ohio.
26. Rice, S. A. (1985) in *Comprehensive chemical kinetics*, vol. 25 (Bamford, C. H., Tipper, C. H. F., Compton, R. G., eds) pp. 3–47, Elsevier Science Publishers, Amsterdam.
27. Davenport, L., Dale, R. E., Bisby, R. H. & Cundall, R. B. (1985) *Biochemistry 24*, 4097–4108.
28. Sklar, A., Miljanich, G. P. & Dratz, E. A. (1979) *Biochemistry 18*, 1707–1716.
29. Lampen, J. E., Arrow, P. M. & Safferman, R. S. (1960) *J. Bacteriol. 80*, 200–206.
30. Sklar, A., Hudson, B. S. & Simoni, R. D. (1977) *Biochemistry 16*, 819–828.
31. Oster, A. (1974) in *Physical methods in chemistry* (Weissberg, B., ed.) pp. 75–117, Wiley Interscience Inc., New York.
32. Paradies, H. H. (1980) *J. Phys. Chem. 84*, 599–607.